ORBITAL STATE UNCERTAINTY REALISM

Joshua T. Horwood and Aubrey B. Poore

Numerica Corporation, 4850 Hahns Peak Drive, Suite 200, Loveland CO, 80538

ABSTRACT

A new class of multivariate probability density functions is proposed called the Gauss von Mises (GVM) family of distributions. The distinguishing feature of the GVM distribution is its definition on a cylindrical manifold, the underlying state space in which systems of orbital element coordinates are more accurately defined, which can provide a statistically rigorous treatment of uncertainty needed for uncertainty propagation and non-linear filtering, orbit determination, tracking, and data association. This paper provides the initial motivation, mathematical background, and definition of the new GVM distribution along with a brief example to illustrate proof-of-concept.

1. INTRODUCTION

Fundamental to the success of the space situational awareness (SSA) mission is the rigorous inclusion of uncertainty in the space surveillance network. The *proper characterization of uncertainty* in the orbital state of a space object is a common requirement to many SSA functions including tracking and data association, resolution of uncorrelated tracks (UCTs), conjunction analysis and probability of collision, sensor resource management, and anomaly detection. While tracking environments, such as air and missile defense, make extensive use of Gaussian and local linearity assumptions within algorithms for uncertainty management, space surveillance is inherently different due to long time gaps between updates, high mis-detection rates, non-linear and non-conservative dynamics, and non-Gaussian phenomena. The latter implies that "covariance realism" is not always sufficient. SSA also needs "uncertainty realism"; the proper characterization of both the state and covariance and all non-zero higher-order cumulants. In other words, a proper characterization of a space object's full state *probability density function (PDF)* is required.

In order to provide a more statistically rigorous treatment of uncertainty in the space surveillance tracking environment and to better support the aforementioned SSA functions, a new class of multivariate PDFs, called *Gauss von Mises (GVM)* distributions, are formulated to more accurately characterize the uncertainty of a space object's state or orbit. Using the new GVM distribution as input, extensions and improvements are possible to key tracking algorithms including a mathematically tractable and operationally viable implementation of the Bayesian non-linear filter used for uncertainty propagation and data fusion, batch processing and orbit determination, and likelihood ratios and other scoring metrics used in data association.

It has been recognized in the space surveillance community that the orbital state uncertainty of a space object can be highly non-Gaussian and statistically robust methods for treating such non-Gaussian uncertainties are sometimes required. Examples of estimation and filtering techniques beyond the traditional extended and unscented Kalman filter, both of which make local linearity and Gaussian assumptions, include Gaussian sum (mixture) filters [1–4], filters based on non-linear propagation of uncertainty using Taylor series expansions of the solution flow [5–7], and particle filters [8]. A drawback of many existing methods for non-linear filtering and uncertainty management, including the ones listed above, is the constraint that the state space be defined on an n-dimensional Cartesian space $\mathbb{R}^n$. Any statistically rigorous treatment of uncertainty must use PDFs defined on the underlying manifold on which the system state is defined. In the space surveillance tracking problem, the system state is often defined with respect to *orbital element coordinates* [9]. In these coordinates, five of the six elements are approximated as unbounded Cartesian coordinates on $\mathbb{R}^5$ while the sixth element is an angular coordinate defined on the circle $\mathbb{S}$ with the angles θ and $\theta + 2\pi k$ (where k is any integer) identified as equivalent (i.e., they describe the same location on the orbit). Thus, more rigorously, an orbital element state space is defined on the six-dimensional cylinder $\mathbb{R}^5 \times \mathbb{S}$. Indeed, the mistreatment of an angular coordinate as an unbounded Cartesian coordinate can lead to many unexpected software faults and other dire consequences as described in Section 2. A key innovation of the GVM distribution is its definition on a *cylindrical state space*

$\mathbb{R}^n \times \mathbb{S}$ with the proper treatment of the angular coordinate within the general framework of directional statistics [10]; hence, the GVM distribution is robust for uncertainty quantification in orbital element space. The Gauss von Mises (GVM) distribution uses the von Mises distribution [10, 11], the analogy of a Gaussian distribution defined on a circle, to robustly describe uncertainty in the angular coordinate. The marginal distribution in the Cartesian coordinates is Gaussian. Additionally, the GVM distribution contains a parameter set controlling the correlation between the angular and Cartesian variables as well as the higher-order cumulants which gives the level sets of the GVM PDF a distinctive "banana" or "boomerang" shape.

By providing a statistically robust treatment of the uncertainty in a space object's orbital element state by rigorously defining the uncertainty on a cylindrical manifold, the GVM distribution supports a suite of next-generation algorithms for uncertainty propagation, data association, space catalog maintenance, and other SSA functions. When adapted to state PDFs modeled by GVM distributions, the general Bayesian non-linear filter is tractable. The prediction step of the resulting GVM filter is made derivative-free, like the UKF, by new quadrature rules for integrating a function multiplied by a GVM weight function, thereby extending the unscented transform [12]. Moreover, prediction using the GVM filter requires the propagation of the same number of sigma points (quadrature nodes) as the standard UKF. Thus, the GVM filter prediction step (uncertainty propagation) has the *same computational cost as the UKF* and, as demonstrated in Section 4 and in future publications, the former can maintain a *proper characterization of the uncertainty* for up to eight times as long as the latter. Additionally, the GVM filter prediction step can make use of a new class of orbital and uncertainty propagators which exploit clusters of nearby states and parallel computer architectures [13, 14]. In the most exceptional cases when the actual state uncertainty deviates from a GVM distribution, a mixture version of the GVM filter can be formulated (using GVM distributions as the mixture components) to ensure proper uncertainty realism in analogy to the Gaussian sum (mixture) filter. Furthermore, the GVM filter is applicable in all regimes of space (e.g., LEO, GEO, HEO) and to both conservative (e.g., gravity) and non-conservative forces (e.g., atmospheric drag, solar radiation pressure). Stochastic process noise, uncertain model parameters, and residual biases can also be treated within the GVM filter using extensions of classical consider analysis and the Schmidt-Kalman filter [15]. A maximum a posteriori batch processing capability for *orbit determination* (track initiation) can also be formulated which generates a GVM PDF characterizing the initial orbital state and uncertainty from a sequence of input reports such as radar, electro-optical, or IR sensor observation data or even full track states. To support the *data fusion* problem of tracking, the correction step of the Bayesian non-linear filter can also be specialized to GVM distributions thereby enabling one to combine reports emanating from a common object to improve the state or understanding of that object. The filter correction step also furnishes a statistically rigorous *prediction error* which appears in the likelihood ratios for scoring the association of one report to another [16]. Thus, the new GVM filter can be used to support *multi-target tracking* within a general multiple hypothesis tracking framework [16, 17]. Additionally, the GVM distribution admits a *distance metric* which extends the classical Mahalanobis distance (χ^2 statistic) [18]. This new "Mahalanobis von Mises" metric provides a test for statistical significance and facilitates validation of the GVM filter. Another noteworthy feature of the GVM framework is its *backwards compatibility* with the space catalog and existing covariance-based algorithms: the GVM distribution reduces to a Gaussian under suitable limits and the GVM filter reduces to the UKF in the case of linear dynamical and measurement models.

It is acknowledged that it is beyond the scope of this paper to address all of the aforementioned topics and justify the many claims stated above. The purpose of this initial paper is to motivate and define the Gauss von Mises (GVM) distribution which will serve as a basis for future publications. The organization of the paper is as follows. Section 2 gives an overview of uncertainty characterization in tracking and discusses coordinate systems used to describe a space object's orbital state and the pitfalls of mistreating an angular coordinate by an unbounded Cartesian coordinate. The von Mises distribution is then introduced as one possible distribution to rigorously treat the uncertainty of an angular variable. Section 3 motivates and defines the GVM distribution. An example demonstrating the use of the GVM distribution in a simulation scenario in LEO is provided in Section 4. Finally, Section 5 provides concluding remarks.

2. UNCERTAINTY ON MANIFOLDS

A permeating theme throughout space situational awareness is the achievement of the correct characterization and management of uncertainty, which in turn is necessary to support conjunction analysis, data association,

anomaly detection, and sensor resource management. The success in achieving a proper characterization of the uncertainty in the state of a space object can depend greatly on the choice of *coordinate system*. Under Gaussian assumptions, the coordinates used to represent the state space can impact how long one can propagate the uncertainty under a non-linear dynamical system; a Gaussian random vector does not get mapped to a Gaussian under a non-linear transformation. The representation of a space object's kinematic state in *orbital element coordinates* [9], rather than Cartesian Earth-Centered-Inertial (ECI) position-velocity coordinates, is well-suited to the space surveillance tracking problem since such coordinates "absorb" the most dominant term in the non-linear gravitational force (i.e., the $1/r^2$ term) leading to "more linear" propagations. Thus, these special coordinates can mitigate the departure from "Gaussianity" under the non-linear propagation of an initial Gaussian state probability density function (PDF) with respect to orbital elements. Additional discussions are provided in Subsection 2.1.

The application of orbital element coordinates within traditional sequential filtering methods such as the extended Kalman filter (EKF), unscented Kalman filter (UKF), and even the highest fidelity Gaussian sum filters has one major disadvantage: the mean anomaly (or mean longitude) angular coordinate describing the location along the orbit is incorrectly treated as an unbounded Cartesian coordinate. Some side effects and pitfalls of such mistreatments within the problems of averaging and fusing angular quantities are described in Subsection 2.2. Ultimately, what is required to rectify these shortcomings is a statistically rigorous treatment of the uncertainty on the *underlying manifold* on which the system state is defined. The theory of directional statistics [10] provides one possible development path. Though the theory can treat uncertainty on very general manifolds (such as tori and hyper-spheres) possessing multiple directional quantities, this work focuses on distributions defined on the circle $\mathbb{S}$ and the $n+1$-dimensional cylinder $\mathbb{R}^n \times \mathbb{S}$. The latter is the manifold on which the orbital element coordinates are more accurately defined. As a starting point, the von Mises PDF [10,11] is introduced in Subsection 2.3 as one possible distribution to rigorously treat the uncertainty of a single angular variable defined on the circle. The von Mises distribution paves the way for the next section concerning the development of the GVM distribution used to represent uncertainty on a cylinder.

2.1 Orbital Element Coordinate Systems

With respect to Cartesian ECI position-velocity coordinates $(\boldsymbol{r}, \dot{\boldsymbol{r}})$, the acceleration $\ddot{\boldsymbol{r}}$ of a space object (e.g., satellite, debris) can be written in the form

$$\ddot{\boldsymbol{r}} = -\frac{\mu_\oplus}{r^3}\boldsymbol{r} + \boldsymbol{a}_{pert}(\boldsymbol{r}, \dot{\boldsymbol{r}}, t). \tag{1}$$

In this equation, $r = |\boldsymbol{r}|$, $\mu_\oplus = GM_\oplus$ where G is the gravitational constant and $M_\oplus$ is the mass of the Earth, and $\boldsymbol{a}_{pert}$ encapsulates all perturbing accelerations of the space object other than those due to the two-body point mass gravitational acceleration.

The *equinoctial orbital elements* [19] (a, h, k, p, q, ℓ) define a system of curvilinear coordinates with respect to six-dimensional position-velocity space. Physical and geometric interpretations of these coordinates as well as the transformation from equinoctial elements to ECI are provided, for example, in Montenbruck and Gill [9]. Models for the perturbing acceleration $\boldsymbol{a}_{pert}$ are also developed in this reference.

The representation of the dynamical model (1) in coordinate systems other than ECI is straightforward to obtain using the chain rule. Indeed, if $\boldsymbol{u} = \boldsymbol{u}(\boldsymbol{r}, \dot{\boldsymbol{r}})$ denotes a coordinate transformation from ECI position-velocity coordinates $(\boldsymbol{r}, \dot{\boldsymbol{r}})$ to a coordinate system $\boldsymbol{u} \in \mathbb{R}^6$ (e.g., equinoctial orbital elements), then (1) is transformed to

$$\dot{\boldsymbol{u}} = \dot{\boldsymbol{u}}_{unpert} + \frac{\partial \boldsymbol{u}}{\partial \dot{\boldsymbol{r}}} \cdot \boldsymbol{a}_{pert}(\boldsymbol{r}, \dot{\boldsymbol{r}}, t), \tag{2}$$

where

$$\dot{\boldsymbol{u}}_{unpert} = \frac{\partial \boldsymbol{u}}{\partial \boldsymbol{r}} \cdot \dot{\boldsymbol{r}} - \frac{\mu_\oplus}{r^3}\frac{\partial \boldsymbol{u}}{\partial \dot{\boldsymbol{r}}} \cdot \boldsymbol{r}. \tag{3}$$

If $\boldsymbol{u}$ is the vector of equinoctial orbital elements, then (3) simplifies to

$$\dot{\boldsymbol{u}}_{unpert} = \left(0, 0, 0, 0, 0, \sqrt{\mu_\oplus / a^3}\right)^T. \tag{4}$$

Therefore, the time evolution of a space object's equinoctial orbital element state (a, h, k, p, q, ℓ) under the assumption of unperturbed two-body dynamics is

$$a(t) = a_0, \quad h(t) = h_0, \quad k(t) = k_0, \quad p(t) = p_0, \quad q(t) = q_0, \quad \ell(t) = \ell_0 + n_0(t - t_0), \tag{5}$$

where $n_0 = \sqrt{\mu_\oplus / a_0^3}$ is the mean motion at the initial epoch.

It is now argued that an equinoctial orbital element state can be regarded as a state defined on the six-dimensional cylinder $\mathbb{R}^5 \times \mathbb{S}$. The definition of the equinoctial orbital elements (a, h, k, p, q, ℓ) implicitly assumes closed (e.g., elliptical) orbits which imposes the following constraints:

$$a > 0, \quad h^2 + k^2 < 1, \quad p, q \in \mathbb{R}, \quad \ell \in \mathbb{S}.$$

Though any real value can be assigned to the mean longitude coordinate ℓ, the angles ℓ and $\ell + 2\pi k$, for any integer $k \in \mathbb{Z}$, define the same location along the orbit; hence ℓ can be regarded as an angular coordinate defined on the circle $\mathbb{S}$. Mathematically, the first five elements (a, h, k, p, q) are not defined everywhere on $\mathbb{R}^5$. Physically however, it can be argued that the sample space in these five coordinates can be approximated as all of $\mathbb{R}^5$. Indeed, the elements (a, h, k, p, q) describe the geometry of the (elliptical) orbit and the orientation of the orbit relative to the equatorial plane. In practice, the uncertainties in the orbital geometry and orientation are sufficiently small so that the probability that an element is close to the constraint boundary is negligible. Moreover, under unperturbed dynamics, these five elements are conserved by Kepler's laws (see Equations (5)) and, consequently, their respective uncertainties do not grow. That said, under the above assumptions, the manifold on which the elements (a, h, k, p, q) are defined can be approximated as all of $\mathbb{R}^5$ and the full six-dimensional equinoctial orbital element state space can be defined on the cylinder $\mathbb{R}^5 \times \mathbb{S}$. With the inclusion of perturbations in the dynamics (e.g., higher-order gravity terms, drag, solar radiation, etc.), the first five elements only evolve with small periodic variations in time and their uncertainties exhibit no long-term secular growth. Thus, the same cylindrical assumptions on the state space apply. These discussions also equally apply to other systems of orbital elements such as Poincaré orbital elements [20], modified equinoctial orbital elements [21], and alternate equinoctial orbital elements [3].

Though the uncertainties in the first five equinoctial elements exhibit only small periodic changes under two-body dynamics, it is the uncertainty along the semi-major axis coordinate a which causes the uncertainty along the mean longitude coordinate ℓ to grow without bound. In other words, as time progresses, one can generally maintain a good understanding of the geometry and orientation of the orbit, but confidence is gradually lost in the exact location of the object along its orbit. The growth in the uncertainty in ℓ can cause undesirable consequences if ℓ is incorrectly treated as an unbounded Cartesian variable or the uncertainty in ℓ is modeled as a Gaussian. With a Gaussian assumption imposed on the PDF in ℓ, one would assign different likelihoods to ℓ and $\ell + 2\pi k$ for different values of $k \in \mathbb{Z}$, even though the mean longitudes ℓ and $\ell + 2\pi k$ define the same location on the circle. Additional insights are provided in the next subsection.

2.2 Examples of Improper Treatments of Angular Quantities

As described in the previous subsection, the mean longitude coordinate (i.e., the sixth equinoctial orbital element) is an angular coordinate in which the angles ℓ and $\ell + 2\pi k$ are identified (equivalent) for any integer $k \in \mathbb{Z}$. In other words, the mean longitude is a circular variable and, as such, a rigorous treatment should not treat it as an unbounded real-valued Cartesian variable. In many cases (and with proper branch cuts defined), it is practical to treat the mean anomaly as real-valued, allowing for distributions to be represented as Gaussians, for example. The drawback of this approach is that the resulting statistics can depend on choice of the integer 'k'.

For example, suppose one wishes to compute the conventional average $\bar{\theta}$ of two angles $\theta_1 = \pi/6$ and $\theta_2 = -\pi/6$. On one hand, $\bar{\theta} = \frac{1}{2}(\theta_1 + \theta_2) = 0$. On the other hand, since $\theta_2 = -\pi/6$ and $\theta_2 = 11\pi/6$ define the same location on the circle, then using this equivalent value of θ_2 in the definition of the average would yield $\bar{\theta} = \pi$. Thus, in order for the conventional average to be well-defined, the statistic

$$\bar{\theta} = \tfrac{1}{2}\big[(\theta_1 + 2\pi k_1) + (\theta_2 + 2\pi k_2)\big] = \tfrac{1}{2}(\theta_1 + \theta_2) + \pi(k_1 + k_2)$$

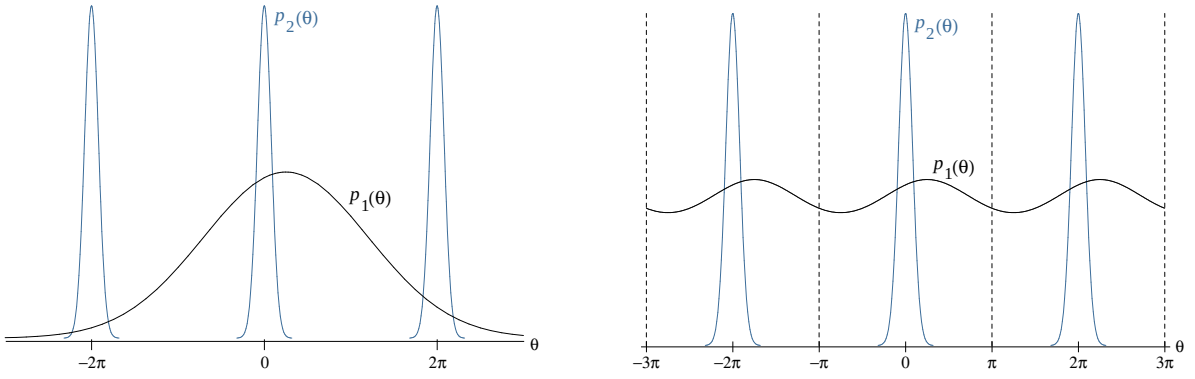

Figure 1. The fusion of a prior PDF $p_1(\theta)$ with an update PDF $p_2(\theta)$ when (a) the angle θ is mis-represented as a Cartesian variable and (b) the angle θ is represented correctly as a circular variable.

must be *independent* of the choice of $k_1, k_2 \in \mathbb{Z}$. Clearly this is not the case for the simple example studied above; different values of k_1 and k_2 can define averages at opposite sides of the circle. The unscented transform used in the UKF can also exhibit similar side effects when used in equinoctial orbital element space (especially if the mean longitude components of the sigma points are sufficiently dispersed) because it requires one to compute a weighted average of angular (mean longitude) components.

A more striking example of the mis-representation of a circular variable as an unbounded Cartesian variable is demonstrated in Figure 1(a). In this simple example, consider a one-dimensional angular state space with two independent states: a "prior" θ_1 and an "update" θ_2 with respective PDFs $p_1(\theta_1)$ and $p_2(\theta_2)$. The PDF in θ_1 (depicted by the black curve) is diffuse (i.e., the uncertainty is large) and, further, θ_1 is incorrectly modeled as an unbounded Cartesian variable. The update state θ_2 (depicted by one of the blue curves) has a mean of zero and a very small variance (uncertainty). Any one of the blue curves can represent the PDF of the update since they are all equivalent up to an integer 2π shift; the "correct" update is *ambiguous*. Within a non-linear filtering application, one might want to fuse the prior θ_1 with the information from θ_2. In such a case, the Bayesian filter correction step yields a "fused PDF" $p_f(\theta)$ in the fused state θ given by

$$p_f(\theta) = \frac{1}{c}\, p_1(\theta)\, p_2(\theta), \quad c = \int_I p_1(\theta)\, p_2(\theta)\, \mathrm{d}\theta, \tag{6}$$

where $I = (-\infty, \infty)$. Thus, the expression obtained for the fused PDF as well as the normalization constant c depend on the choice (i.e., 2π shift) of the update PDF. In particular, a mis-computed normalization constant c can have severe consequences within a tracking system, as analogous expressions for c appear in the likelihood ratios for scoring the association of one report to another [16]. Figure 1(b) depicts how these ambiguity issues can be resolved by turning to the theory of directional statistics. Further analysis is provided in the next subsection.

2.3 von Mises Probability Density Function

The source of the ambiguity in computing the fused PDF (6) in the example of the previous subsection lies in the incorrect treatment of an angular variable as an unbounded Cartesian real-valued variable. These problems can be rectified by representing the state PDF not necessarily on a Cartesian space $\mathbb{R}^n$ but instead on the manifold that more accurately describes the global topology of the underlying state space. The most important change needed for (equinoctial) orbital element states is the representation of the uncertainty in the angular coordinate (mean longitude) as a PDF on the circle $\mathbb{S}$ so that the joint PDF in the six orbital elements defines a distribution on the cylinder $\mathbb{R}^5 \times \mathbb{S}$. In order to do so, PDFs defined on the circle are required.

A function $p : \mathbb{R} \to \mathbb{R}$ is a probability density function (PDF) on the circle $\mathbb{S}$ if and only if [10]

1. $p(\theta) \geqslant 0$ almost everywhere on $(-\infty, \infty)$,
2. $p(\theta + 2\pi) = p(\theta)$ almost everywhere on $(-\infty, \infty)$,

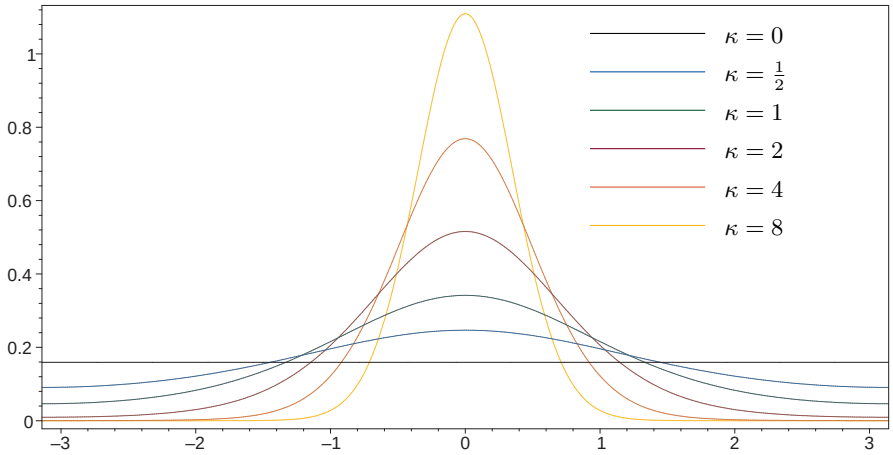

Figure 2. The von Mises probability density function (7) with location parameter $\alpha = 0$ and various values of the concentration parameter κ.

3. $\int_{-\pi}^{\pi} p(\theta)\,\mathrm{d}\theta = 1$.

One example satisfying the above conditions is the *von Mises distribution* which provides an analogy of a Gaussian distribution defined on a circle. The von Mises PDF in the angular variable θ is defined by [10, 11]

$$\mathcal{VM}(\theta; \alpha, \kappa) = \frac{\mathrm{e}^{\kappa \cos(\theta - \alpha)}}{2\pi I_0(\kappa)}, \tag{7}$$

where I_0 is the modified Bessel function of the first kind of order 0. The parameters μ and κ are measures of location and concentration. As $\kappa \to 0^+$, the von Mises distribution tends to a uniform distribution. For large κ, the von Mises distribution becomes concentrated about the angle α and approaches a Gaussian distribution in θ with mean μ and variance $1/\kappa$. Some example plots are shown in Figure 2. An algebraically equivalent expression of (7) which is numerically stable for large values of κ is

$$\mathcal{VM}(\theta; \alpha, \kappa) = \frac{\mathrm{e}^{-2\kappa \sin^2 \frac{1}{2}(\theta - \alpha)}}{2\pi \mathrm{e}^{-\kappa} I_0(\kappa)}. \tag{8}$$

The von Mises distribution (8) is used in the next section to construct the Gauss von Mises distribution defined on the cylinder $\mathbb{R}^n \times \mathbb{S}$.

This section concludes with a discussion on how the von Mises distribution can resolve the problems in the previous subsection concerning the averaging and fusion of angular quantities. Suppose $\theta_1, \ldots, \theta_N$ is a sample of independent observations coming from a von Mises distribution. Then, the maximum likelihood estimate of the location parameter α is

$$\hat{\alpha} = \arg\left(\frac{1}{N} \sum_{j=1}^{N} \mathrm{e}^{\mathrm{i}\theta_j} \right). \tag{9}$$

Unlike the conventional average $(\theta_1 + \cdots + \theta_N)/N$, the "average" $\hat{\alpha}$ is *independent* of any 2π shift in the angles θ_j. In the fusion example, if the prior and update PDFs are von Mises distributions, i.e.,

$$p_1(\theta_1) = \mathcal{VM}(\theta_1; \alpha_1, \kappa_1), \quad p_2(\theta_2) = \mathcal{VM}(\theta_2; \alpha_2, \kappa_2),$$

then the fused PDF (6) can be formed unambiguously and $p_f(\theta) = p_f(\theta + 2\pi k)$ for any $k \in \mathbb{Z}$. As seen in Figure 1(b), there is no longer any ambiguity in how to choose the "correct" update PDF $p_2(\theta)$, since both $p_1(\theta)$ and $p_2(\theta)$ are properly defined circular PDFs. The integration interval I in the computation of the normalization constant c in (6) is any interval of length 2π; i.e., $I = (a, a + 2\pi)$ for some $a \in \mathbb{R}$. In other words, the value of c is independent of the choice of a.

3. CONSTRUCTION OF THE GAUSS VON MISES DISTRIBUTION

This section defines the Gauss von Mises (GVM) distribution used to characterize the uncertainty in a space object's orbital state. The proposed GVM distribution is not defined as a function of other random variables with specified probability density functions (PDFs). Instead, its construction is based on satisfying the following requirements listed below.

1. The GVM family of multivariate PDFs is defined on the $n+1$-dimensional cylindrical manifold $\mathbb{R}^n \times \mathbb{S}$.
2. The GVM distribution has a sufficiently general parameter set which can model non-zero higher-order cumulants beyond a usual "mean" and "covariance."
3. The GVM distribution can account for correlation between the Cartesian random vector $\boldsymbol{x} \in \mathbb{R}^n$ and the circular random variable $\theta \in \mathbb{S}$.
4. The level sets of the GVM distribution are generally "banana" or "boomerang" shaped so that a more accurate characterization of the uncertainty in a space object's state in equinoctial orbital elements can be achieved.
5. The GVM distribution reduces to a multivariate Gaussian PDF in a suitable limit.
6. The GVM distribution permits a tractable implementation of the general Bayesian non-linear filter and other applications needed to support advanced SSA.

In clarification of the first requirement, a function $p : \mathbb{R}^n \times \mathbb{R} \to \mathbb{R}$ is a probability density function (PDF) on the cylinder $\mathbb{R}^n \times \mathbb{S}$ if and only if

1. $p(\boldsymbol{x}, \theta) \geqslant 0$ almost everywhere on $\mathbb{R}^n \times \mathbb{R}$,
2. $p(\boldsymbol{x}, \theta + 2\pi) = p(\boldsymbol{x}, \theta)$ almost everywhere on $\mathbb{R}^n \times \mathbb{R}$,
3. $\int_{\mathbb{R}^n} \int_{-\pi}^{\pi} p(\boldsymbol{x}, \theta) \, \mathrm{d}\theta \, \mathrm{d}\boldsymbol{x} = 1$.

This definition extends the definition of a PDF defined on a circle (see §3.2 of Reference [10]). One example satisfying the above conditions is

$$p(\boldsymbol{x}, \theta) = \mathcal{N}(\boldsymbol{x}; \boldsymbol{\mu}, \mathbf{P}) \, \mathcal{VM}(\theta; \alpha, \kappa),$$

where $\mathcal{VM}(\theta; \alpha, \kappa)$ is the von Mises PDF defined by (8) and $\mathcal{N}(\boldsymbol{x}; \boldsymbol{\mu}, \mathbf{P})$ is the multivariate Gaussian PDF given by

$$\mathcal{N}(\boldsymbol{x}; \boldsymbol{\mu}, \mathbf{P}) = \frac{1}{\sqrt{\det(2\pi\mathbf{P})}} \exp\left[-\frac{1}{2}(\boldsymbol{x} - \boldsymbol{\mu})^T \mathbf{P}^{-1} (\boldsymbol{x} - \boldsymbol{\mu})\right], \tag{10}$$

where $\boldsymbol{\mu} \in \mathbb{R}^n$ and $\mathbf{P}$ is an $n \times n$ symmetric positive-definite (covariance) matrix. This simple example, though used as a starting point in constructing the GVM distribution, does not satisfy all of the requirements listed earlier. In particular, the desired family of multivariate PDFs needs to model correlation between $\boldsymbol{x}$ and θ and have level sets possessing a distinctive banana or boomerang shape.

To motivate the construction of the GVM distribution, consider two random vectors $\boldsymbol{x} \in \mathbb{R}^n$ and $\boldsymbol{y} \in \mathbb{R}^m$ whose joint PDF is Gaussian:

$$p(\boldsymbol{x}, \boldsymbol{y}) = \mathcal{N}\left(\begin{bmatrix}\boldsymbol{x}\\ \boldsymbol{y}\end{bmatrix}; \begin{bmatrix}\boldsymbol{\mu}_x\\ \boldsymbol{\mu}_y\end{bmatrix}, \begin{bmatrix}\mathbf{P}_{xx} & \mathbf{P}_{yx}^T\\ \mathbf{P}_{yx} & \mathbf{P}_{yy}\end{bmatrix}\right). \tag{11}$$

Using the definition of conditional probability and the *Schur complement decomposition*, the joint PDF (11) can be expressed as

$$\begin{aligned} p(\boldsymbol{x}, \boldsymbol{y}) &= p(\boldsymbol{x}) \, p(\boldsymbol{y}|\boldsymbol{x}) \\ &= \mathcal{N}(\boldsymbol{x}; \boldsymbol{\mu}_x, \mathbf{P}_{xx}) \, \mathcal{N}(\boldsymbol{y}; \boldsymbol{\mu}_y + \mathbf{P}_{yx}\mathbf{P}_{xx}^{-1}(\boldsymbol{x} - \boldsymbol{\mu}_x), \mathbf{P}_{yy} - \mathbf{P}_{yx}\mathbf{P}_{xx}^{-1}\mathbf{P}_{yx}^T) \\ &\equiv \mathcal{N}(\boldsymbol{x}; \boldsymbol{\mu}_x, \mathbf{P}_{xx}) \, \mathcal{N}(\boldsymbol{y}; \boldsymbol{g}(\boldsymbol{x}), \mathbf{Q}), \end{aligned} \tag{12}$$

where

$$\boldsymbol{g}(\boldsymbol{x}) = \boldsymbol{\mu}_y + \mathbf{P}_{yx}\mathbf{P}_{xx}^{-1}(\boldsymbol{x} - \boldsymbol{\mu}_x), \quad \mathbf{Q} = \mathbf{P}_{yy} - \mathbf{P}_{yx}\mathbf{P}_{xx}^{-1}\mathbf{P}_{yx}^T.$$

One very powerful observation resulting from this Schur complement decomposition is that (12) defines a PDF in $(\boldsymbol{x}, \boldsymbol{y})$ for *any* (analytic) function $\boldsymbol{g}(\boldsymbol{x})$ and *any* symmetric positive-definite matrix $\mathbf{Q}$. In particular, if $\boldsymbol{y}$ is univariate and relabelled as θ, then

$$p(\boldsymbol{x}, \theta) = \mathcal{N}(\boldsymbol{x}; \boldsymbol{\mu}_x, \mathbf{P}_{xx})\, \mathcal{N}(\theta; \Theta(\boldsymbol{x}), \kappa),$$

defines a PDF on $\mathbb{R}^n \times \mathbb{R}$ for any analytic function $\Theta : \mathbb{R}^n \to \mathbb{R}$ and any positive scalar κ. To make it robust for a *circular variable* $\theta \in \mathbb{S}$ and hence define a PDF on the cylinder $\mathbb{R}^n \times \mathbb{S}$, we replace the Gaussian PDF in θ by the von Mises PDF in θ:

$$p(\boldsymbol{x}, \theta) = \mathcal{N}(\boldsymbol{x}; \boldsymbol{\mu}_x, \mathbf{P}_{xx})\, \mathcal{VM}(\theta; \Theta(\boldsymbol{x}), \kappa). \tag{13}$$

The definition of the Gauss von Mises distribution fixes the specific form of the function $\Theta(\boldsymbol{x})$ in (13) so that the PDF can model non-zero higher-order cumulants (i.e., the banana shape of the level sets) but is not overly complicated so as the make the resulting Bayesian filter prediction and correction steps intractable.

Definition [Gauss von Mises (GVM) Distribution] The random variables $(\boldsymbol{x}, \theta) \in \mathbb{R}^n \times \mathbb{S}$ are said to be jointly distributed as a *Gauss von Mises (GVM) distribution* if and only if their joint probability density function has the form

$$\begin{aligned} p(\boldsymbol{x}, \theta) &= \mathcal{GVM}(\boldsymbol{x}, \theta; \boldsymbol{\mu}, \mathbf{P}, \alpha, \boldsymbol{\beta}, \boldsymbol{\Gamma}, \kappa) \\ &\equiv \mathcal{N}(\boldsymbol{x}; \boldsymbol{\mu}, \mathbf{P})\, \mathcal{VM}(\theta; \Theta(\boldsymbol{x}), \kappa), \end{aligned}$$

where

$$\begin{aligned} \mathcal{N}(\boldsymbol{x}; \boldsymbol{\mu}, \mathbf{P}) &= \frac{1}{\sqrt{\det(2\pi\mathbf{P})}} \exp\left[-\frac{1}{2}(\boldsymbol{x} - \boldsymbol{\mu})^T \mathbf{P}^{-1}(\boldsymbol{x} - \boldsymbol{\mu})\right], \\ \mathcal{VM}(\theta; \Theta(\boldsymbol{x}), \kappa) &= \frac{1}{2\pi \mathrm{e}^{-\kappa} I_0(\kappa)} \exp\left[-2\kappa \sin^2 \frac{1}{2}\big(\theta - \Theta(\boldsymbol{x})\big)\right], \end{aligned}$$

and

$$\Theta(\boldsymbol{x}) = \alpha + \boldsymbol{\beta}^T \boldsymbol{z} + \tfrac{1}{2}\boldsymbol{z}^T \boldsymbol{\Gamma} \boldsymbol{z}, \quad \boldsymbol{z} = \mathbf{A}^{-1}(\boldsymbol{x} - \boldsymbol{\mu}), \quad \mathbf{P} = \mathbf{A}\mathbf{A}^T.$$

The parameter set $(\boldsymbol{\mu}, \mathbf{P}, \alpha, \boldsymbol{\beta}, \boldsymbol{\Gamma}, \kappa)$ is subject to the following constraints: $\boldsymbol{\mu} \in \mathbb{R}^n$, $\mathbf{P}$ is an $n \times n$ symmetric positive-definite matrix, $\alpha \in \mathbb{R}$, $\boldsymbol{\beta} \in \mathbb{R}^n$, $\boldsymbol{\Gamma}$ is an $n \times n$ symmetric matrix, and $\kappa \geqslant 0$. The matrix $\mathbf{A}$ in the definition of the normalized variable $\boldsymbol{z}$ is the lower-triangular Cholesky factor of the parameter matrix $\mathbf{P}$.

It is noted that the function $\Theta(\boldsymbol{x})$ appearing in the GVM distribution is an inhomogeneous quadratic in $\boldsymbol{x}$ or, equivalently, the normalized variable $\boldsymbol{z}$. The use of the normalized variable $\boldsymbol{z}$ in the definition is made to simplify the ensuing mathematics and so that the parameters $\boldsymbol{\beta}$ and $\boldsymbol{\Gamma}$ are dimensionless. Additionally, the parameters $\boldsymbol{\beta}$ and $\boldsymbol{\Gamma}$ model correlation between $\boldsymbol{x}$ and θ. The parameter matrix $\boldsymbol{\Gamma}$ can be tuned to give the level sets of the GVM distribution their distinctive banana or boomerang shape. Future publications will demonstrate that the definition of the GVM distribution satisfies the remaining requirements listed at the beginning of the section.

4. EXAMPLE

To briefly demonstrate the implication of mis-characterizing orbital uncertainty and the improvements obtained when using the Gauss von Mises (GVM) distribution, Figure 3 compares the uncertainty propagation algorithms implicit in the extended Kalman filter (EKF), unscented Kalman filter (UKF), and new GVM filter. (Full details of the latter will be provided in a future publication.) The initial conditions considered in this example describe a circular, non-inclined orbit in LEO with a semi-major axis (SMA) of 7136.635 km and SMA standard deviation of 20 km. Figure 3(a) shows a particle representation of the initial orbital state PDF in equinoctial orbital element space [19] plotted on the semi-major axis–mean longitude plane. The particles are dispersed according to the level curves ranging from 0.5 to 3 sigmas in half sigma increments. Figure 3(b) shows the results of propagating

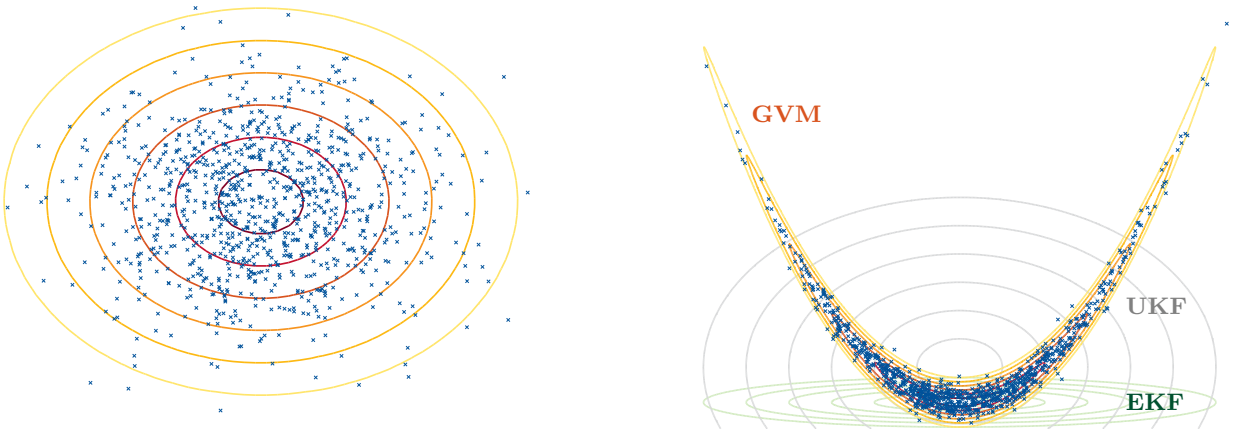

(a) Initial Gaussian representation of the uncertainty

(b) Propagated uncertainty using the EKF, UKF, GVM filter, and a particle filter

Figure 3. Illustration of uncertainty characterization during orbital propagation.

this initial uncertainty (for eight orbital periods in this example) using the EKF, UKF, and GVM filter. The respective level curves of the PDF computed from the EKF, UKF, and GVM filter are superimposed on the figure. Clearly, the level curves computed from the GVM filter capture the actual uncertainty characterized by the particle ensemble. For the UKF, its covariance (depicted by the grey ellipsoidal level curves) is indeed realistic in the sense that it agrees with that computed from the definition of the covariance using the true PDF. Thus, in this example, the UKF provides "covariance realism" but clearly does not support "uncertainty realism" since the covariance does not represent the actual banana-shaped uncertainty of the true PDF. Further, the state estimate produced from the UKF coincides with the mean of the true PDF; however the mean is displaced from the mode of the true PDF. Consequently, the probability that the object is within a small neighborhood centered at the UKF state estimate (mean) is essentially zero. The EKF, on the other hand, provides a state estimate coinciding closely with the mode of the true PDF, but the covariance tends to collapse making inflation necessary to begin to cover the uncertainty. In neither the EKF nor UKF case does the covariance actually model the uncertainty. This example illustrates the problem of using a single Gaussian PDF (i.e., covariance) to represent uncertainty and suggests that the GVM distribution provides a better representation of the actual orbital state PDF which is needed if one is to achieve statistically robust characterization of uncertainty, which again is fundamental to achieving a robust capability across the SSN.

5. CONCLUSIONS

This paper provided the initial motivation, mathematical background, and definition of a new class of multivariate probability density functions, called the Gauss von Mises (GVM) distribution, which provides a statistically rigorous treatment of a space object's uncertainty in an orbital element space. In future publications, it will be shown how the new GVM distribution and its resulting applications can support some of the future needs of the SSA mission by providing advanced algorithms for data fusion, orbit determination, tracking, and uncertainty propagation. Of particular significance is the GVM uncertainty propagation algorithm which will be shown to have the same computational cost as the traditional unscented Kalman filter with the former able to maintain uncertainty realism for up to eight times as long as the latter. In conjunction with the new orbital and uncertainty propagator of Aristoff and Poore [13, 14], the GVM framework can provide a next-generation *uncertainty management package* for space surveillance.

ACKNOWLEDGMENTS

The research described in this paper was funded in part by a grant (FA9550-11-1-0248) and a Phase II STTR (FA9550-12-C-0034) from the Air Force Office of Scientific Research.

REFERENCES

1. G. Terejanu, P. Singla, T. Singh, and P. D. Scott, "Uncertainty propagation for nonlinear dynamic systems using Gaussian mixture models," *Journal of Guidance, Control and Dynamics*, vol. 31, no. 6, pp. 1623–1633, 2008.
2. J. T. Horwood and A. B. Poore, "Adaptive Gaussian sum filters for space surveillance," *IEEE Transactions on Automatic Control*, vol. 56, no. 8, pp. 1777–1790, 2011.
3. J. T. Horwood, N. D. Aragon, and A. B. Poore, "Gaussian sum filters for space surveillance: theory and simulations," *Journal of Guidance, Control, and Dynamics*, vol. 34, no. 6, pp. 1839–1851, 2011.
4. K. J. DeMars, M. K. Jah, Y. Cheng, and R. H. Bishop, "Methods for splitting Gaussian distributions and applications within the AEGIS filter," in *Proceedings of the 22nd AAS/AIAA Space Flight Mechanics Meeting*, (Charleston, SC), February 2012. Paper AAS-12-261.
5. R. S. Park and D. J. Scheeres, "Nonlinear mapping of Gaussian statistics: theory and applications to spacecraft trajectory design," *Journal of Guidance, Control, and Dynamics*, vol. 29, no. 6, pp. 1367–1375, 2006.
6. R. S. Park and D. J. Scheeres, "Nonlinear semi-analytic methods for trajectory estimation," *Journal of Guidance, Control, and Dynamics*, vol. 30, no. 6, pp. 1668–1676, 2007.
7. K. Fujimoto and D. J. Scheeres, "Non-linear propagation of uncertainty with non-conservative effects," in *Proceedings of the 22nd AAS/AIAA Space Flight Mechanics Meeting*, (Charleston, SC), February 2012. Paper AAS-12-263.
8. B. Ristic, S. Arulampalam, and N. Gordon, *Beyond the Kalman Filter: Particle Filters for Tracking Applications*. Boston: Artech House, 2004.
9. O. Montenbruck and E. Gill, *Satellite Orbits: Models, Methods, and Applications*. Berlin: Springer, 2000.
10. K. V. Mardia and P. E. Jupp, *Directional Statistics*. New York: John Wiley & Sons, 2000.
11. K. V. Mardia, "Algorithm AS 86: The von Mises distribution function," *Applied Statistics*, vol. 24, pp. 268–272, 1975.
12. S. J. Julier, J. K. Uhlmann, and H. F. Durant-Whyte, "A new method for the nonlinear transformation of means and covariances in filters and estimators," *IEEE Transactions on Automatic Control*, vol. 55, pp. 477–482, 2000.
13. J. M. Aristoff and A. B. Poore, "Implicit Runge-Kutta methods for orbit propagation," in *Proceedings of the 2012 AAS/AIAA Astrodynamics Specialist Conference*, (Minneapolis, MN), August 2012.
14. J. M. Aristoff and A. B. Poore, "Implicit Runge-Kutta methods for uncertainty propagation," in *Proceedings of the 2012 Advanced Maui Optical and Space Surveillance Technologies Conference*, (Wailea, HI), September 2012.
15. A. H. Jazwinski, *Stochastic Processes and Filtering Theory*. New York: Dover, 1970.
16. A. B. Poore, "Multidimensional assignment formulation of data association problems arising from multitarget tracking and multisensor data fusion," *Computational Optimization and Applications*, vol. 3, pp. 27–57, 1994.
17. D. B. Reid, "An algorithm for tracking multiple targets," *IEEE Transactions on Automatic Control*, vol. 24, no. 6, pp. 843–854, 1997.
18. P. C. Mahalanobis, "On the generalised distance in statistics," *Proceedings of the National Institute of Sciences of India*, vol. 2, no. 1, pp. 49–55, 1936.
19. R. A. Broucke and P. J. Cefola, "On the equinoctial orbit elements," *Celestial Mechanics*, vol. 5, pp. 303–310, 1972.
20. R. H. Lyddane, "Small eccentricities or inclinations in the Brouwer theory of the artificial satellite," *Astronomical Journal*, vol. 68, pp. 555–558, 1963.
21. M. J. H. Walker, B. Ireland, and J. Owens, "A set of modified equinoctial orbit elements," *Celestial Mechanics*, vol. 36, pp. 409–419, 1985.